Supplementary Information (SI) for Sustainable Energy & Fuels.

SUPPORTING INFORMATION

Enhancing kerosene selectivity in Fischer-Tropsch synthesis with ceria-coated catalysts

M. Amine Lwazzani[1]; Andrés A. García Blanco[1]; Martí Biset-Peiró[1]; Elena Martín-Morales[1]; Jordi Guilera[1,2*]

[1] Catalonia Institute for Energy Research (IREC), Jardins de Les Dones de Negre 1, 08930, Sant Adrià de Besòs, Spain

[2] Facultat de Química, Universitat de Barcelona, Martí i Franquès, 1, Barcelona 08028, Spain

[*] Corresponding author. E-mail adress: jguilera@irec.cat

Characterization

SEM:

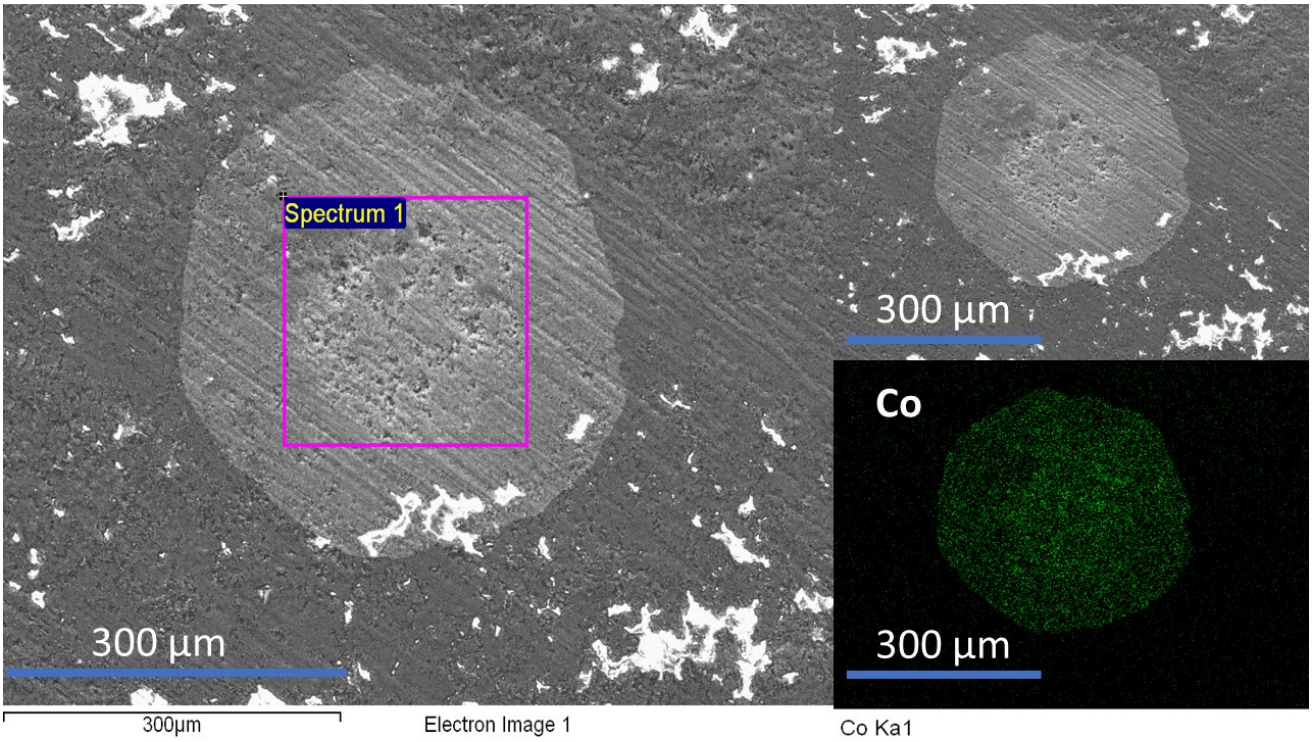

Figure S.1: (Left) Cross-Section of the Co catalyst under electronic microscopy. (Right) Mapping of the Co presence in the same catalyst particle and SEM image.

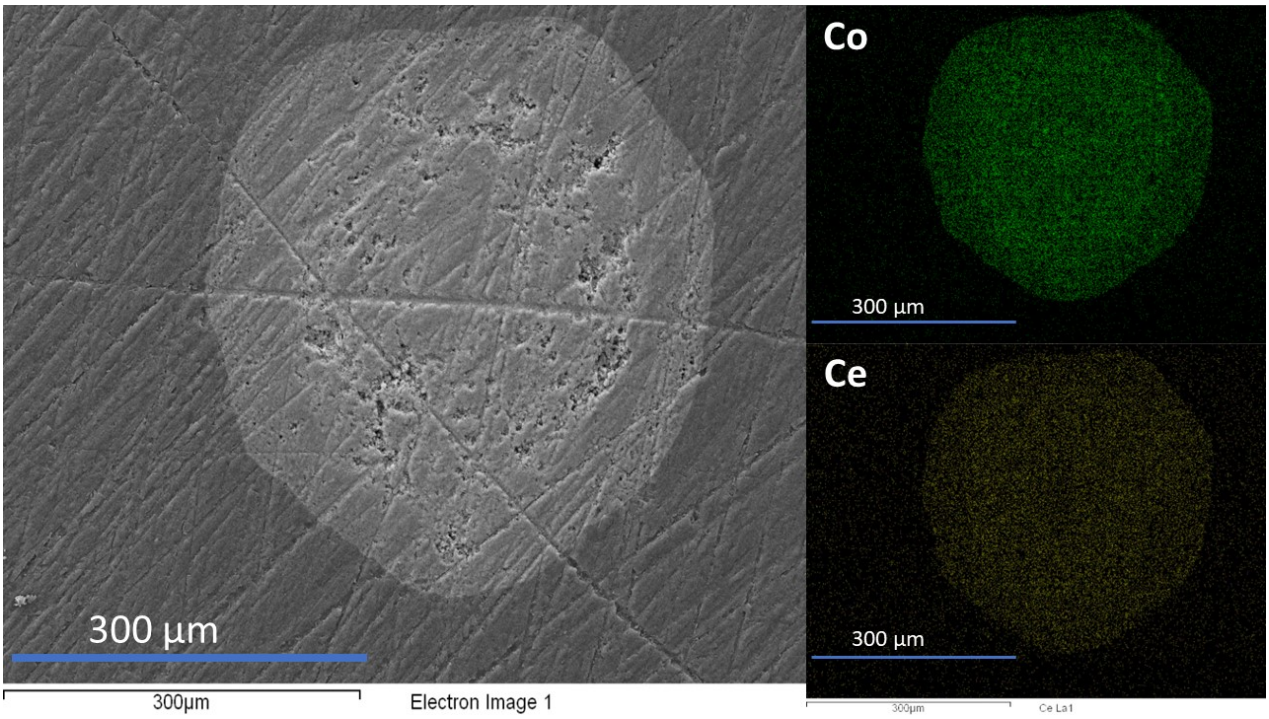

Figure S.2: (Left) Cross-Section of the CoCe catalyst under electronic microscopy. (Right) Mapping of the Co and Ce presence in the same catalyst particle.

N_2-physisorption:

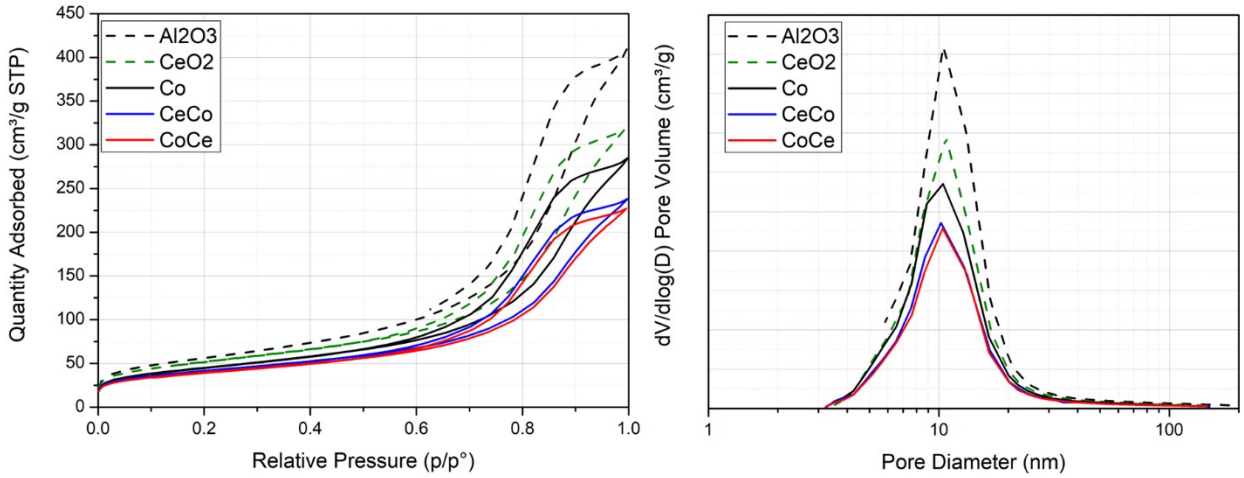

Figure S.3: (Left) N2 adsorption-desorption isotherms. (Right) Pore Diameter of the Catalysts.

Figure S.3 shows the nitrogen adsorption-desorption isotherms and the pore size distribution of the γ-Al_2O_3 support and catalysts evaluated in the present work. All samples showed a mesoporous-type isotherm [1–4], without noticeable nitrogen adsorption in the micropore range. Cerium incorporation on reference did not cause any change in the isotherm shape. The mesopore size distribution of cerium-promoted catalysts slightly shifted to lower values than those of reference. This fact is a direct consequence of the promoter incorporation, which reduced the dimensions of the largest pores. There were no differences between promoted catalysts.

XRD:

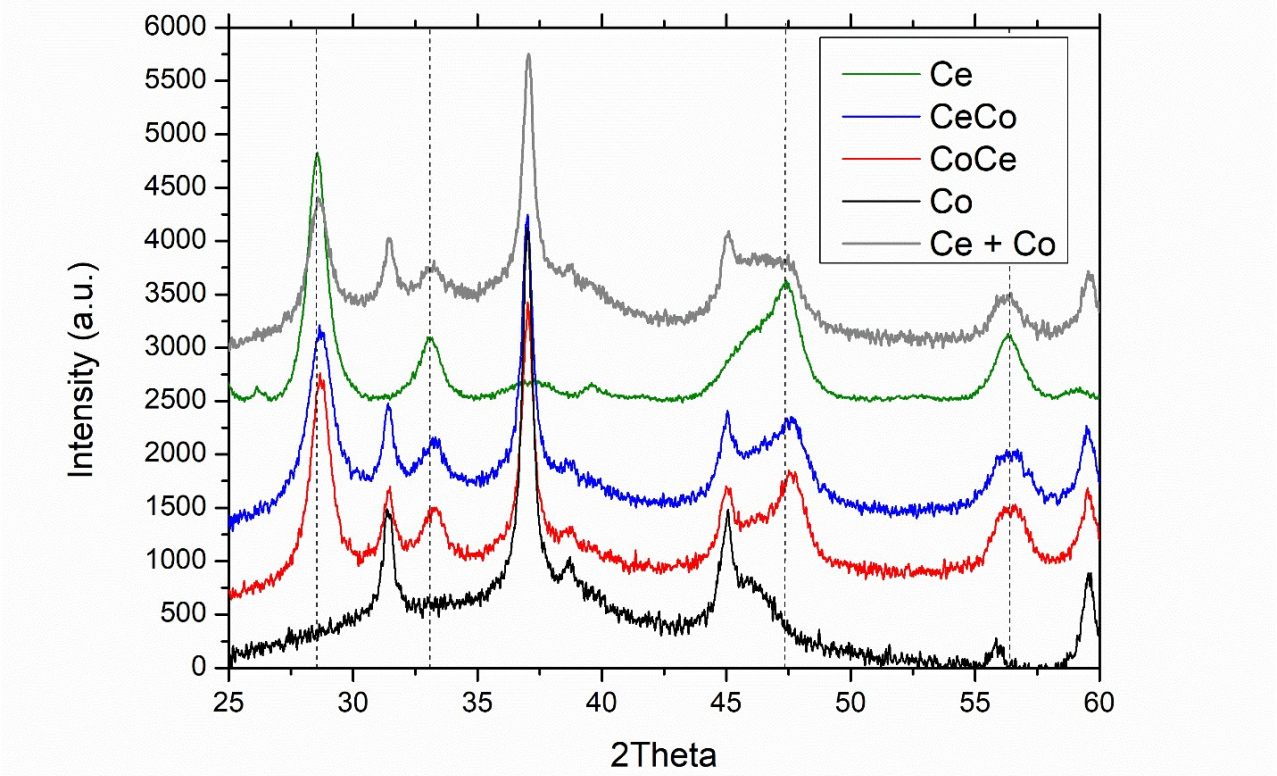

Figure S. 4: CeO2 XRD lattice shifts

New XRD measurements were made focusing in the 25-60 º range to better visualize the presence in the ceria lattice shifts, which are shown in Figure S. 4. The peaks from the Ce material, (Ce/γ-Al_2O_3 , 10%) deviate from the Ce-Co materials, as they show slight deviations towards higher 2Theta values. To avoid experimental errors, a sample was prepared by combining the Co and Ce catalyst powders, as the cobalt peaks remained fix in the cobalts samples, to evaluate possible experimental deviations, thereby eliminating the possibility of measurement error.

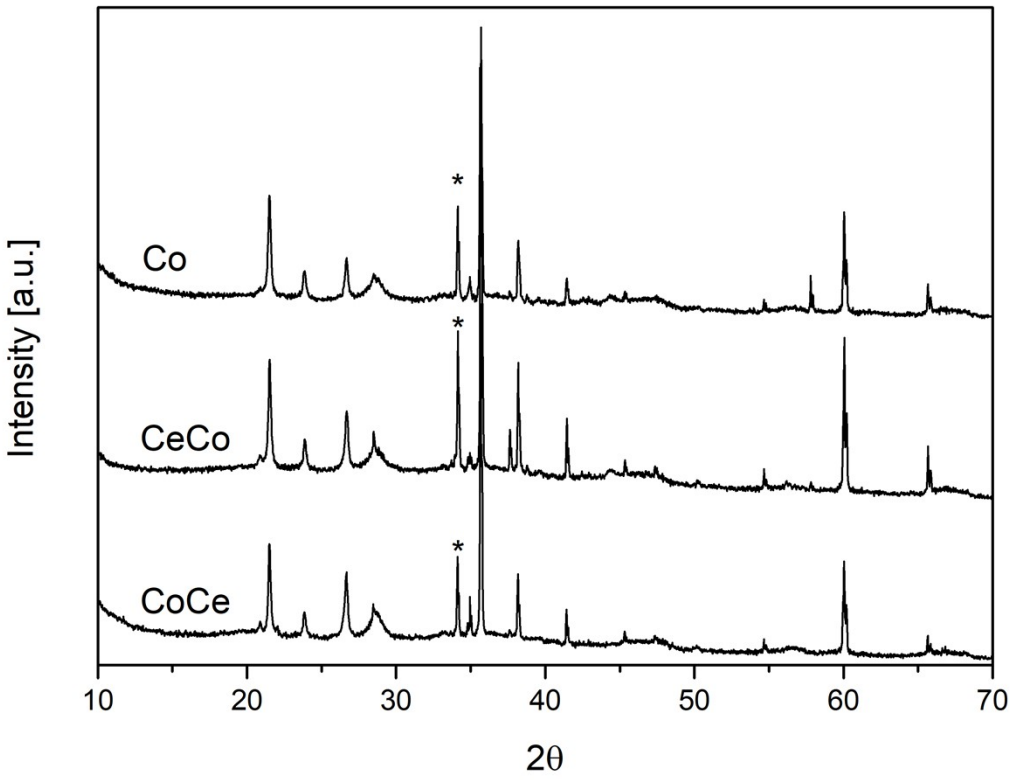

Figure S.5: XRD diffractograms of the catalysts used in this work post to reaction.

In Figure S.4. The symbol (*) represents the peak [2θ=34.15º] corresponding to CoO (ICDD 00-042-1300). No other peaks were highlighted because the silicon compounds and the cerium aluminate caused them. The absence of peaks related to Co_3O_4 indicates that the reduction has been effective, and no relevant peaks are indicating the formation of cobalt aluminates, although this may be also since they can be amorphous[5,6]. The presence of CoO can be explained by a re-oxidation of the metallic Cobalt upon interaction with the ambient oxygen.

TPR:

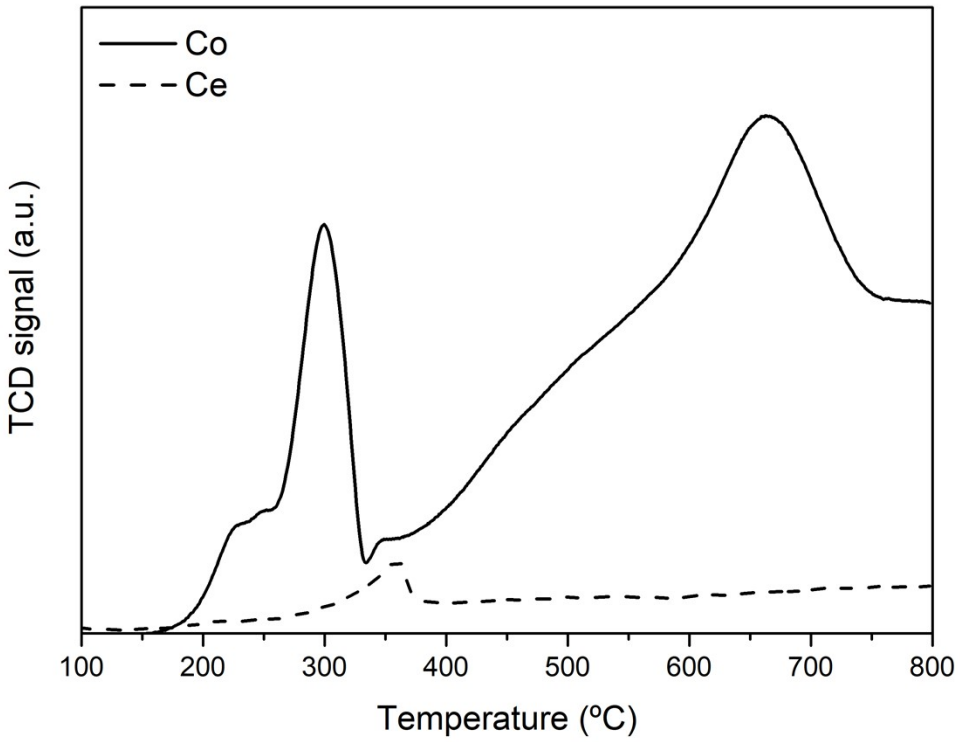

Figure S.6: TPR profiles of the Co reference catalyst and Ce.

In Figure S5, shows the TPR profiles of the Co catalyst, used as a reference, and impregnated ceria. It is observed that ceria is hardly reduced in comparison to the other catalysts, also its reduction takes place at higher temperatures. Curiously, the high-temperature reduction peak observed in the promoted catalyst is not observed with the Ce material (Ce/γ-Al_2O_3), which may be due to interactions of the ceria-cobalt species.

CO Chemisorption:

Table S.1: Adsorbed mols of CO of the catalytic materials under CO Chemisorption.

Cat.	Co	CeCo	CoCe	Ce
Mass of sample (g). at 500 ºC	0.096	0.090	0.104	0.044
Volume Adsorbed (cm^3) at 500 ºC	0.834	0.713	0.908	0.013
Mass of sample (g). at 380 ºC	0.094	0.099	0.92	-
Volume Adsorbed (cm^3). at 380 ºC	0.646	0.387	0.370	-

Table S.1 represents the obtained values of Chemisorbed CO on the catalytic materials, from this table it can be inferred that the impregnated ceria material is not active for CO adsorption when compared to the rest of the catalysts.Table S. 2: CO Chemisorption values at 380 ºC and 500 ºC of the catalysts.

Catalyst	Co	CoCe	CeCo
Metallic Surface Area ($m^2 \cdot g^{-1}$) At 500ºC	1.5	1.6	1.3
Metallic Dispersion (%) At 500ºC	1.5	1.6	1.2
Metallic Surface Area ($m^2 \cdot g^{-1}$) At 380ºC	1.1	0.6	0.6
Metallic Dispersion (%) At 380ºC	1.1	0.6	0.6
Dispersion ratio (380 ºC/500 ºC)	0.71	0.39	0.47

The CO chemisorption at 380 ºC and 500 ºC reveals different adsorption behaviors of the catalysts, as at 380 ºC the ceria promoted catalysts show similar results, below the unpromoted catalyst. Contrarly to what was obtained at 380 ºC, results after reduction at 500 ºC, showed similar or even slightly enhanced CO Chemisorption of the CoCe catalyst respective to the Co reference materials and superior to the CeCo catalyst. This phenomenon was explained in the main document due to restrained reduction of the ceria-containing catalysts.

XPS

XPS spectra for Co 2p is shown in below in Figure 7.

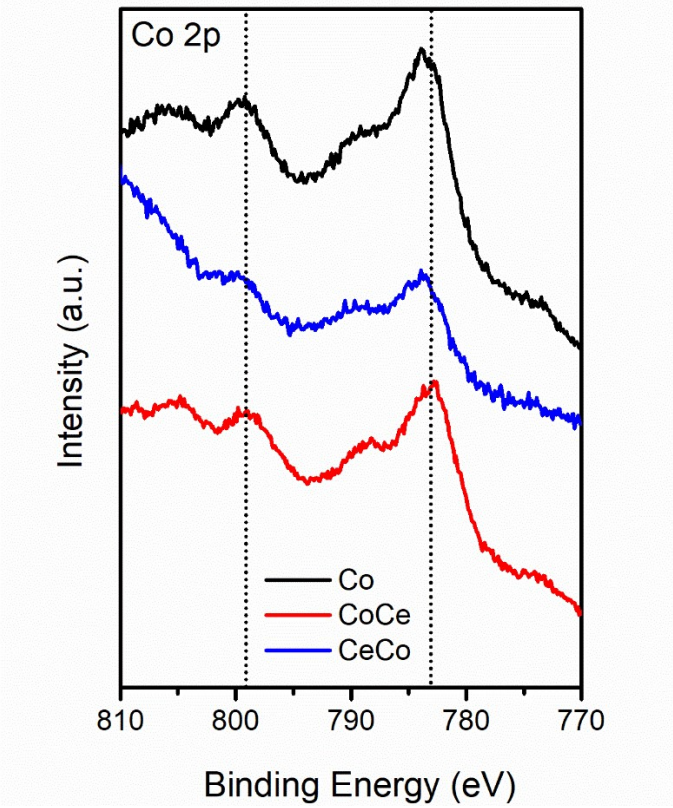

Figure S. 7: XPS spectra for Co 2p.

Catalytic Results

Table S.3: Catalytic Results of the reference Catalyst under H_2/CO and H_2/CO/CO_2

Catalyst	Temperature [ºC]	Conversion CO	Conversion H_2	Conversion CO_2	GHSV [NmL·h^{-1}·g^{-1}]	Selectivity CH_4	Selectivity C_2-C_4	Selectivity C_5-C_9	Selectivity C_9-C_{17}	Selectivity C_{18+}	α
Co/	230	52	54	-	5,290	11	5	18	36	30	0.95
H_2/CO	245	47	51	-	8,464	20	10	16	31	24	0.95
	260	52	58	-	11,286	32	16	14	25	13	0.94
Co/	230	47	51	5.4	3,937	15	12	20	33	20	0.94
H_2/CO/CO_2	245	48	54	1.7	5,765	19	10	20	34	17	0.94
	260	50	60	-3.7	8,085	33	15	16	23	12	0.93

Table S.4: Catalytic results of the Cerium-promoted catalysts under syngas.

Cat.	Temperature [ºC]	Conversion [%] CO	Conversion [%] H_2	GHSV [NmL·g^{-1}·h^{-1}]	Selectivity [%] CH_4	Selectivity [%] C_2-C_4	Selectivity [%] C_5-C_9	Selectivity [%] C_9-C_{17}	Selectivity [%] C_{18+}	α α_1	α α_2
CeCo	230	48	48	2800	5	8	15	45	28	0.98	0.93
	245	47	48	4200	10	5	17	40	28	0.96	0.93
	260	55	59	5600	26	13	17	28	16	0.94	0.92
CoCe	230	45	49	4509	9	3	17	43	28	0.96	0.90
	245	42	45	7215	22	9	18	33	17	0.94	0.87
	260	50	56	9619	28	13	20	28	11	0.94	0.87

Table S.5: Catalytic results of Ceria promoted catalysts under CO_2-rich mixture.

Cat.	Temperature [ºC]	Conversion [%] CO	Conversion [%] H_2	Conversion [%] CO_2	GHSV [NmL·g^{-1}·h^{-1}]	Selectivity [%] CH_4	Selectivity [%] C_2-C_4	Selectivity [%] C_5-C_9	Selectivity [%] C_9-C_{17}	Selectivity [%] C_{18+}	α α_1	α α_2
CeCo	230	46	50	-2.7	2120	12	5	16	46	22	0.97	0.91
	245	51	60	-7.9	3041	23	7	12	40	18	0.98	0.90
	260	47	64	-34.9	4322	40	13	13	22	12	0.94	0.90
CoCe	230	54	57	6.2	3143	10	8	19	42	21	0.96	0.90
	245	54	61	1.2	4607	22	7	13	41	18	0.94	0.87
	260	62	71	-7.2	6486	34	13	17	25	11	0.94	0.87

Table S.6: CO_2 selectivity for the promoted catalysts.

CO_2 Selectivity [%]			
Temperature	Cat.		
[ºC]	Co	CeCo	CoCe
230	0.2	0.2	0.4
245	0.6	0.4	0.8
260	1.6	1.1	1.8

Table S. 7: Catalytic Activity (CTY).

Cat.	Temperature [ºC]	mcat [g]	Co mass [g Co]	XCO [%]	Flux [NmL·min^{-1}]	Flux [mol syngas·min^{-1}]	Flux [Mol Co/s]	CTY [mol CO·s^{-1}·g Co^{-1}]
				SYNGAS				
Co	230	0.425	0.06	52	37.5	1.53E-03	8.53E-06	14.03
	245	0.425	0.06	47	60	2.46E-03	1.36E-05	22.45
	260	0.425	0.06	52	80	3.27E-03	1.82E-05	29.93
CoCe	230	0.499	0.07	45	37.5	1.53E-03	8.53E-06	11.78
	245	0.499	0.07	42	60	2.46E-03	1.36E-05	18.85
	260	0.499	0.07	50	80	3.27E-03	1.82E-05	25.14
CeCo	230	0.428	0.07	48	20	8.18E-04	4.55E-06	6.94
	245	0.428	0.07	47	30	1.23E-03	6.82E-06	10.42
	260	0.428	0.07	55	40	1.64E-03	9.09E-06	13.89
				SYNGAS + CO_2				
Co	230	0.426	0.06	47	28	1.15E-03	6.37E-06	10.45
	245	0.426	0.06	48	41	1.68E-03	9.32E-06	15.30
	260	0.426	0.06	50	57.5	2.35E-03	1.31E-05	21.46
CoCe	230	0.507	0.07	54	26.6	1.09E-03	6.05E-06	8.23
	245	0.507	0.07	54	39	1.60E-03	8.87E-06	12.06
	260	0.507	0.07	62	54.6	2.23E-03	1.24E-05	16.89
CeCo	230	0.651	0.10	46	23	9.41E-04	5.23E-06	5.25
	245	0.651	0.10	51	33	1.35E-03	7.50E-06	7.53
	260	0.651	0.10	47	46.9	1.92E-03	1.07E-05	10.71

Table S. 8: Average value and standard deviation for catalyst conversion.

Cat.	Temperature [ºC]	Reactant	Mean	Std. Dev.	Sample nº	95% Error margin
			SYNGAS			
Co	230	CO	52.35	1.03	10	0.73
		H_2	54.15	0.82	10	0.59
	245	CO	46.79	0.44	11	0.30
		H_2	50.52	0.73	11	0.49
	260	CO	52.09	0.26	9	0.20
		H_2	58.49	0.38	9	0.29
CoCe	230	CO	46.13	3.48	9	2.68
		H_2	43.70	4.31	9	3.31
	245	CO	41.92	1.05	7	0.97
		H_2	45.24	1.03	7	0.96
	260	CO	50.90	2.28	6	2.39
		H_2	56.55	2.51	6	2.64
CeCo	230	CO	46.01	0.37	13	0.22
		H_2	49.65	0.31	13	0.19
	245	CO	50.79	0.63	11	0.42
		H_2	59.65	1.00	11	0.67
	260	CO	46.16	1.36	7	1.26
		H_2	63.54	1.44	7	1.33
			SYNGAS + CO2			
Co	230	CO	47.92	0.77	36	0.26

		H_2	50.98	0.57	36	0.19
	245	CO	47.86	0.51	13	0.31
		H_2	54.41	0.39	13	0.24
	260	CO	49.54	0.61	9	0.47
		H_2	59.66	0.26	9	0.20
CoCe	230	CO	53.59	1.04	13	0.63
		H_2	56.61	0.81	13	0.49
	245	CO	53.96	0.23	7	0.21
		H_2	61.02	0.37	7	0.34
	260	CO	61.75	1.05	7	0.97
		H_2	71.25	0.64	7	0.59
CeCo	230	CO	47.61	1.54	28	0.60
		H_2	48.16	1.52	28	0.59
	245	CO	46.50	0.82	11	0.55
		H_2	48.08	0.87	11	0.58
	260	CO	54.98	0.41	11	0.28
		H_2	59.20	0.47	11	0.32

Isoparaffin, Olefin and alcohols:

Table S. 9: Isoparaffin, olefin and alcohol content of the C5+ hydrocarbons.

Cat	Temperature	Total				Within the Kerosene range (C_9-C_{17})	
				SYNGAS			
Cat	Tª (ºC)	Paraffins	Iso-Paraffins	Olefins	Alcohols	Iso-Paraffins	Olefins
Co	230	99.13	0.03	0.62	0.30	100.00	100.00
Co	245	99.28	0.01	0.14	0.72	100.00	49.19
Co	260	97.97	0.00	1.28	0.85	-	96.19
CeCo	230	97.56	0.08	2.00	0.58	83.50	98.10
CeCo	245	98.24	0.09	1.78	1.59	0.00	98.88
CeCo	260	97.49	0.00	1.43	1.09	-	100.00
CoCe	230	97.12	0.40	1.65	0.83	100.00	100.00
CoCe	245	96.60	0.38	2.26	0.76	100.00	100.00
CoCe	260	97.42	0.12	2.14	0.73	100.00	98.23
				SYNGAS + CO_2			
Co	230	96.03	0.39	2.91	0.68	100.00	100.00
Co	245	96.32	0.37	3.25	0.12	100.00	91.85
Co	260	94.47	0.90	4.62	0.39	88.81	99.16
CeCo	230	96.95	0.39	2.28	0.39	100.00	100.00
CeCo	245	99.15	0.40	0.00	0.45	100.00	-

CeCo	260	97.83	0.56	0.96	0.84	100.00	100.00
CoCe	230	98.00	0.00	1.21	0.80	-	91.85
CoCe	245	91.38	4.00	3.92	1.22	86.26	95.02
CoCe	260	99.10	1.71	2.67	0.90	73.00	100.00

Time On Stream (TOS):

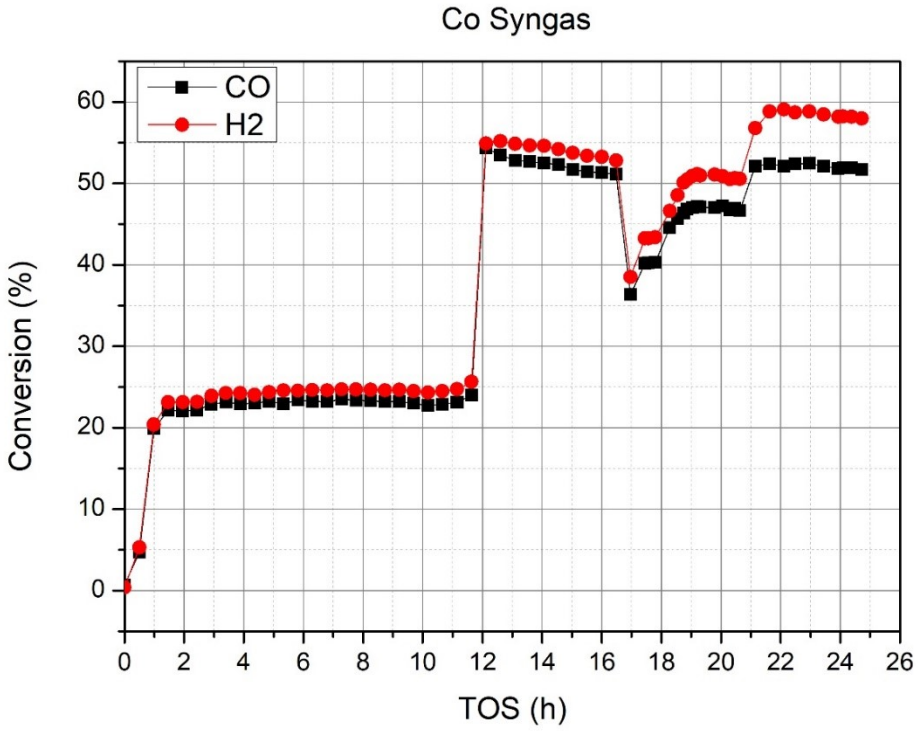

Figure S. 8: TOS for the Co catalyst under syngas.

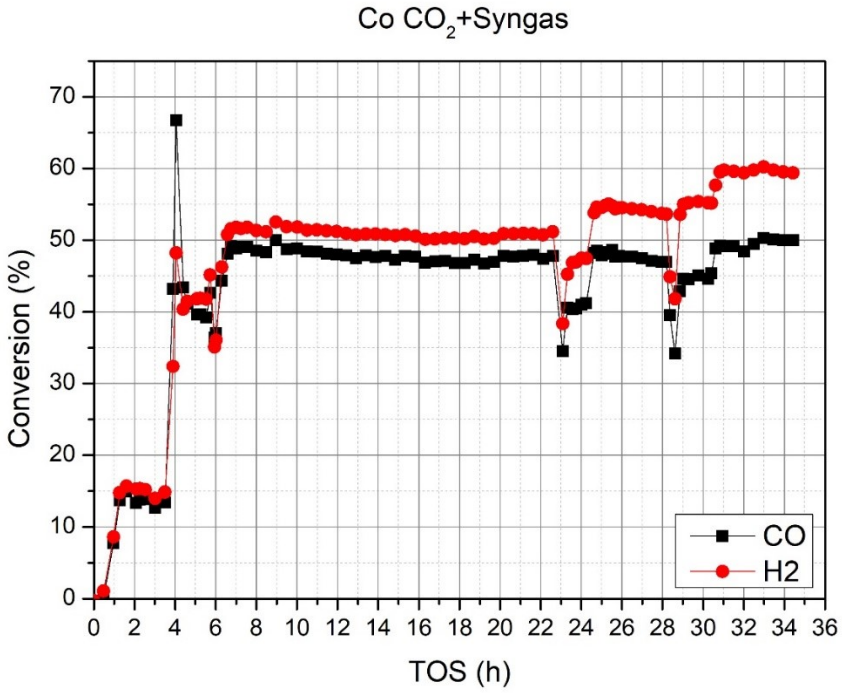

Figure S. 9: TOS for the Co catalyst under CO2-enriched syngas.

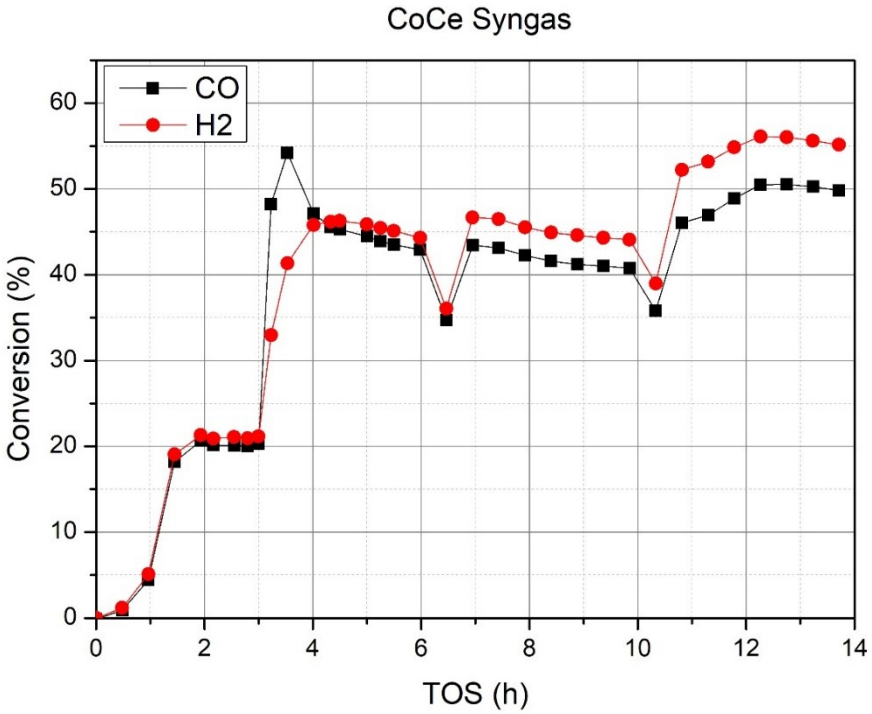

Figure S. 10: TOS for the CoCe catalyst under syngas.

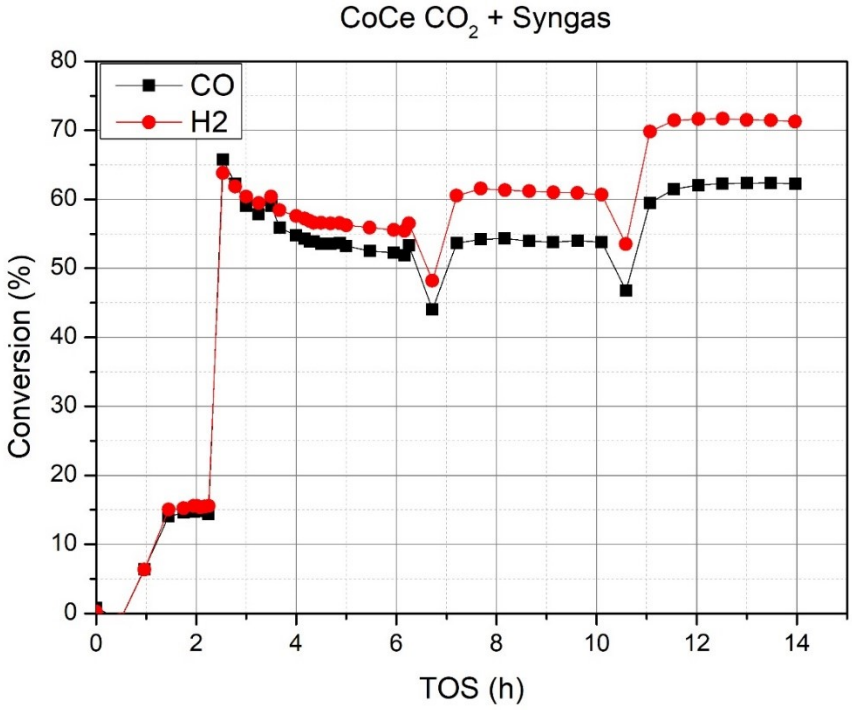

Figure S. 11: TOS for the CoCe catalyst under CO2-enriched syngas.

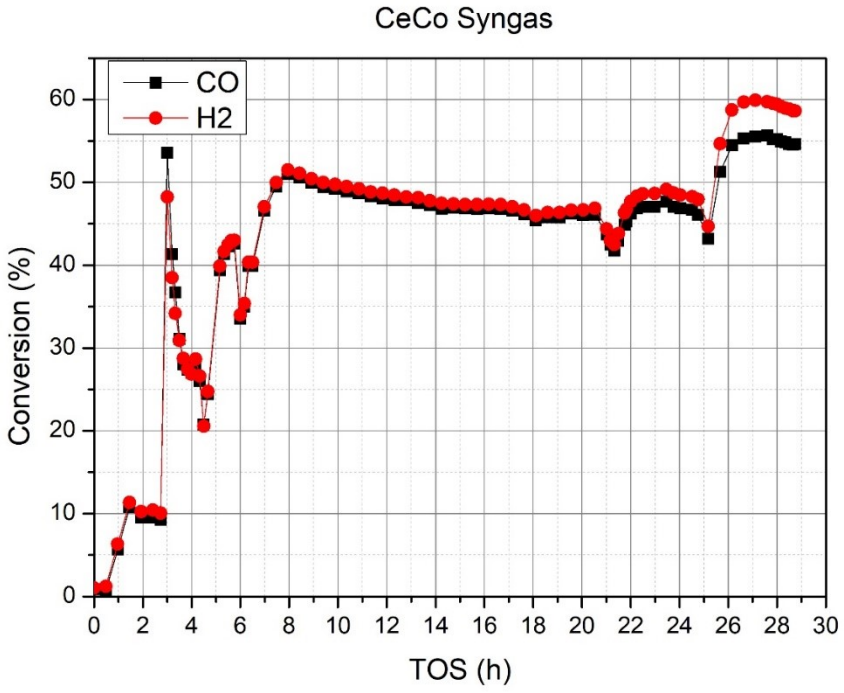

Figure S. 12: TOS for the CeCo catalyst under syngas.

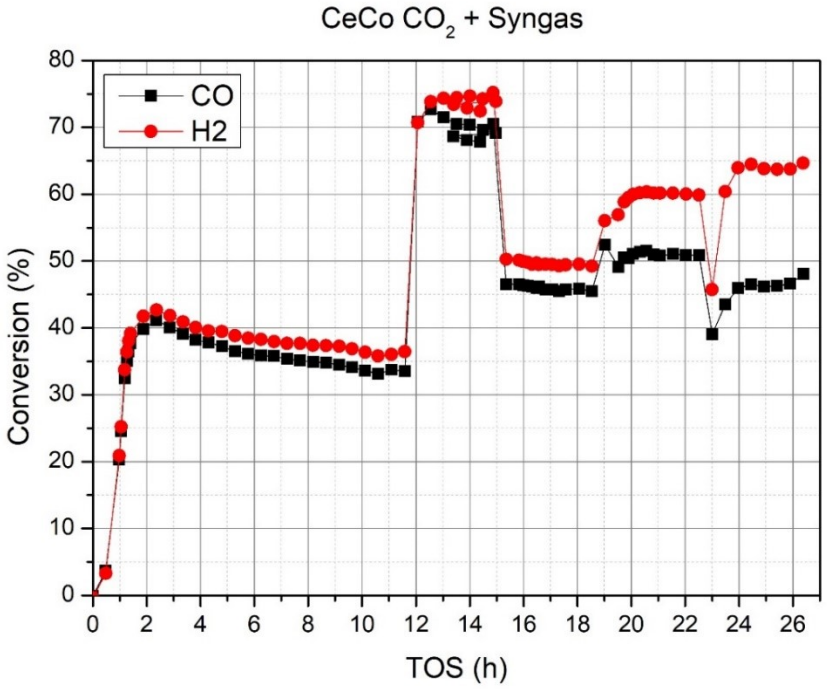

Figure S. 13: TOS for the CeCo catalyst under CO2-enriched syngas.

DRIFT:

DRIFT characterization was also performed under CO_2 feed to understand the adsorption behavior and the changes in the adsorbate species while undergoing reaction-like conditions. The obtained results are shown in Figure S. 13 and Figure S. 14:

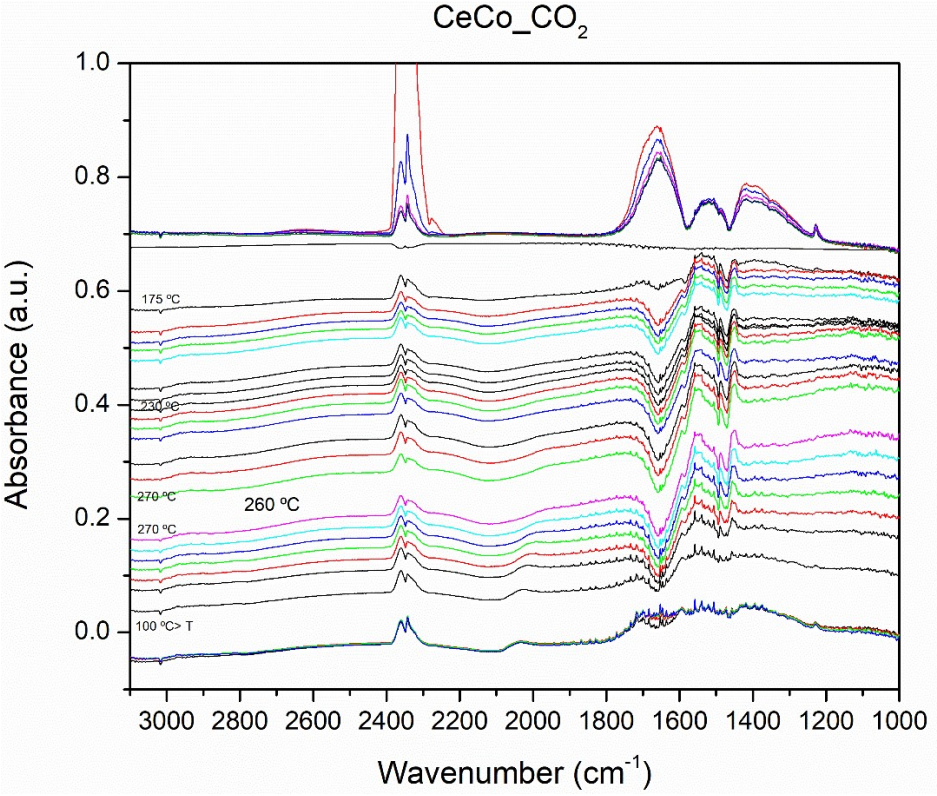

Figure S. 14: DRIFT characterization of the CeCo catalyst under CO_2 hydrogenation.

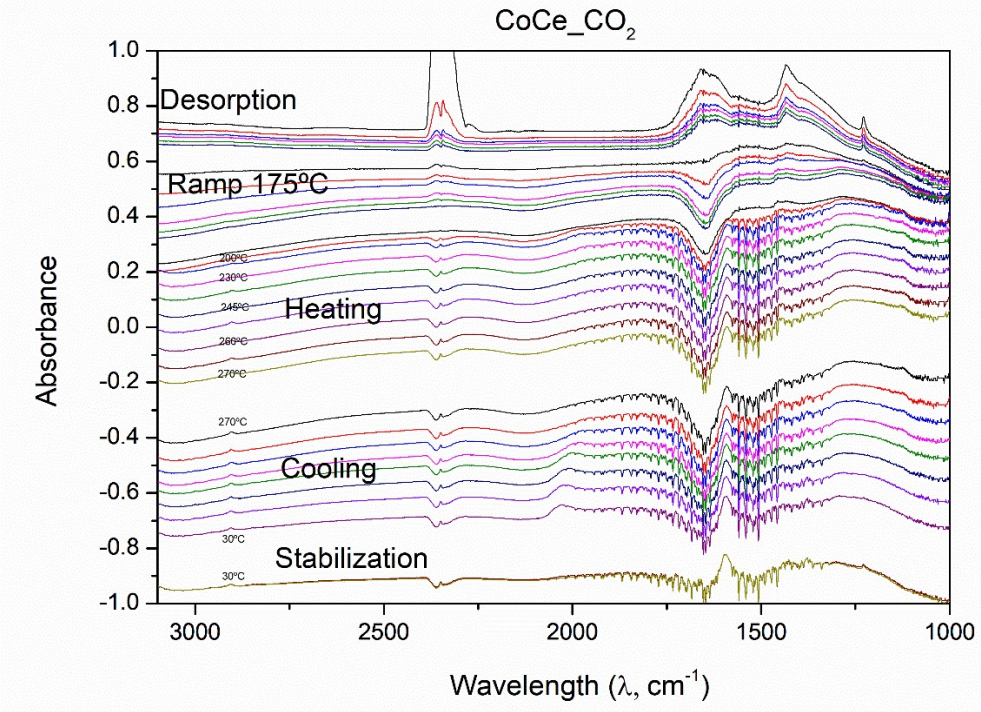

Figure S. 15: DRIFT characterization of the CoCe catalyst under CO_2 hydrogenation.

Relative areas of the DRIFT peaks were quantified by measuring the area of each peak, relative to the linearly adsorbed CO peak (2022 cm^{-1}).

Table S. 10: IR peak assignment, and relative areas in reference to linear CO absorption band 2022 cm^{-1}

Peak (cm-1)	**Adsorbate species**	**Co**	**CoCe**	**CeCo**
3762 - 3665	Hydroxyls [7–9]	20.6%	36.7%	6.1%
3016	Hydrocarbons [10]	13.6%	3.6%	3.6%
2901	Formate [10]	2.3%	6.9%	13.8%
2835	Formate [11]	6.0%	23.7%	9.0%
2022	Linear Carbonyl [8–10]	100%	100%	100%
1930	Multiply-bonded carbonyl [10]	14.4%	57.5%	8.8%
1868	Bridged Carbonyl [10]	27.3%	166.8%	42.5%
1590	Carbonate [9,10]	69.6%	200.6%	88.0%
1374	Carbonate [9,10]	19.8%	47.1%	1.2%

The areas used for estimating the values corresponding to each adsorbate species was calculated as seen in Figure S. 13.

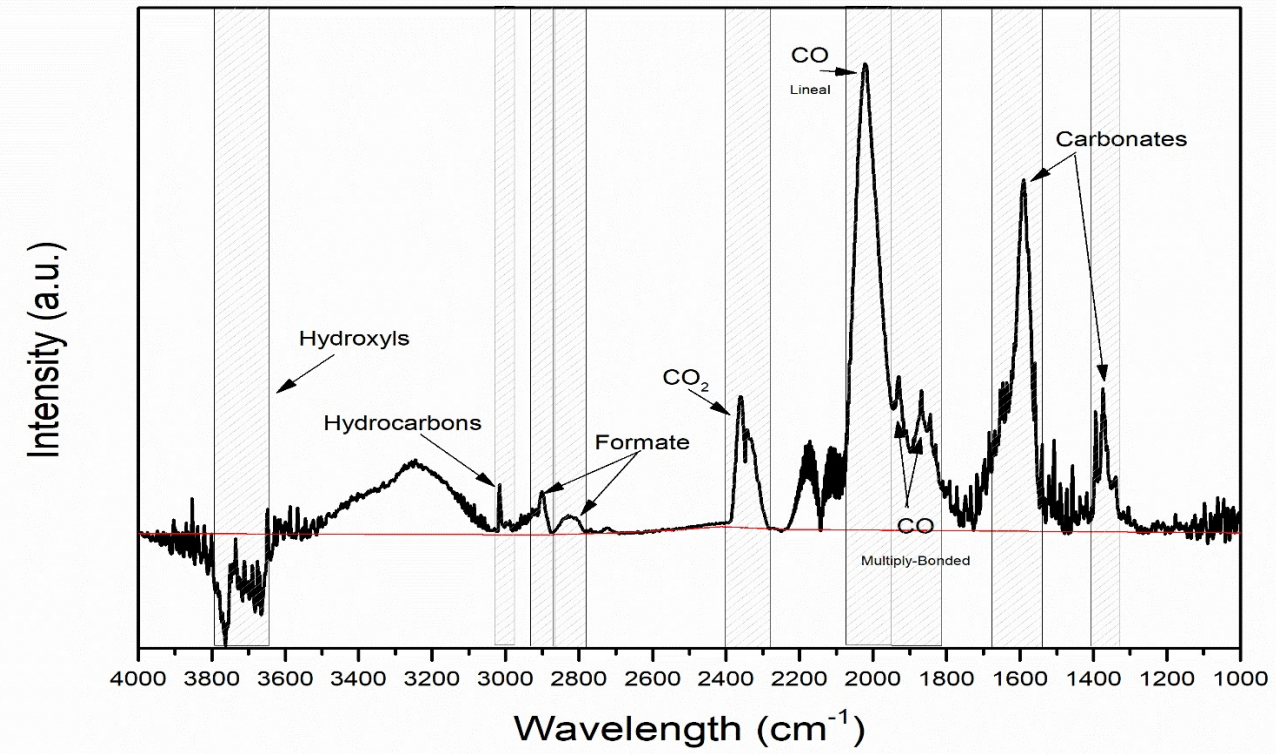

Figure S. 16: DRIFT area delimitation.

Table S. 11: Ratio of Bridged CO to linear CO, and ratio of surface carbonates to surface carbonyls, calculated using the relative areas of Table S.9

	Co	*CoCe*	*CeCo*
Bridged CO / linear CO	*0.42*	*2.24*	*0.51*
Carbonates/carbonyls	*0.63*	*0.76*	*0.59*

***R*eferences:**

[1] R. Haul, S. J. Gregg, K. S. W. Sing: Adsorption, Surface Area and Porosity. 2. Auflage, Academic Press, London 1982. 303 Seiten, Preis: $ 49.50, Berichte Der Bunsengesellschaft Für Physikalische Chemie 86 (1982) 957–957. https://doi.org/10.1002/bbpc.19820861019.

[2] F. Rouquerol, J. Rouquerol, K. Sing, CHAPTER 7 - Assessment of Mesoporosity, in: F. Rouquerol, J. Rouquerol, K. Sing (Eds.), Adsorption by Powders and Porous Solids, Academic Press, London, 1999: pp. 191–217. https://doi.org/10.1016/B978-012598920-6/50008-7.

[3] M. Thommes, Physical Adsorption Characterization of Nanoporous Materials, Chemie Ingenieur Technik 82 (2010) 1059–1073. https://doi.org/10.1002/cite.201000064.

[4] M. Thommes, K. Kaneko, A.V. Neimark, J.P. Olivier, F. Rodriguez-Reinoso, J. Rouquerol, K.S.W. Sing, Physisorption of gases, with special reference to the evaluation of surface area and pore size distribution (IUPAC Technical Report), Pure and Applied Chemistry 87 (2015) 1051–1069. https://doi.org/10.1515/pac-2014-1117.

[5] N.M. Deraz, Formation and Characterization of Cobalt Aluminate Nano-Particles, International Journal of Electrochemical Science 8 (2013) 4036–4046. https://doi.org/10.1016/S1452-3981(23)14451-8.

[6] E.M. Masoud, A.-A. El-Bellihi, W.A. Bayoumy, E.S. Abdelazeem, Structural, optical, magnetic, and electrical properties of nanospinels containing different molar ratios of cobalt and aluminum ions, Ionics 23 (2017) 2417–2427. https://doi.org/10.1007/s11581-017-2091-0.

[7] X. Liu, DRIFTS Study of Surface of γ-Alumina and Its Dehydroxylation, J. Phys. Chem. C 112 (2008) 5066–5073. https://doi.org/10.1021/jp711901s.

[8] L.F. Bobadilla, A. Egaña, R. Castillo, F. Romero-Sarria, M.A. Centeno, O. Sanz, M. Montes, J.A. Odriozola, Understanding the promotional effect of Pt/CeO2 in cobalt-catalyzed Fischer-Tropsch synthesis using *operando* infrared spectroscopy at moderated pressures, Fuel 312 (2022) 122964. https://doi.org/10.1016/j.fuel.2021.122964.

[9] P.A.U. Aldana, F. Ocampo, K. Kobl, B. Louis, F. Thibault-Starzyk, M. Daturi, P. Bazin, S. Thomas, A.C. Roger, Catalytic CO2 valorization into CH4 on Ni-based ceria-zirconia. Reaction mechanism by operando IR spectroscopy, Catalysis Today 215 (2013) 201–207. https://doi.org/10.1016/j.cattod.2013.02.019.

[10] C.G. Visconti, L. Lietti, E. Tronconi, P. Forzatti, R. Zennaro, E. Finocchio, Fischer–Tropsch synthesis on a Co/Al2O3 catalyst with CO2 containing syngas, Applied Catalysis A: General 355 (2009) 61–68. https://doi.org/10.1016/j.apcata.2008.11.027.

[11] A. Parastaev, V. Muravev, E. Huertas Osta, A.J.F. Van Hoof, T.F. Kimpel, N. Kosinov, E.J.M. Hensen, Boosting CO2 hydrogenation via size-dependent metal–support interactions in cobalt/ceria-based catalysts, Nat Catal 3 (2020) 526–533. https://doi.org/10.1038/s41929-020-0459-4.

Annex 1. Reference Catalyst Optimization

Before ceria promotion, a reference cobalt catalyst was optimized by modifying impregnated metal content, calcination temperature, and impregnation steps, results are shown below:

Table S.12: Description of the catalysts: Composition and procedural parameters.

Cat. ID	Description
10A	10 wt% cobalt supported over γ -Al_2O_3 calcined at 500ºC.
10B	10 wt% cobalt supported over γ -Al_2O_3 calcined at 275ºC.
14B	14 wt% cobalt supported over γ -Al_2O_3 calcined at 275ºC.
14A	14 wt% cobalt supported over γ -Al_2O_3 calcined at 500ºC.
17.5A1	17.5 wt% cobalt supported over γ -Al_2O_3 calcined at 500ºC and impregnated in one step.
17.5A3	17.5 wt% cobalt supported over γ -Al_2O_3 calcined at 500ºC and impregnated in 3 steps.
17.5Bi	17.5 wt% cobalt supported over γ -Al_2O_3 calcined at 275ºC, impregnated in 3 steps with intermediate calcination between every impregnation.
17.5B1	17.5 wt% cobalt supported over γ -Al_2O_3 calcined at 275ºC impregnated in one step.

The series of catalyst samples obtained are described in Table S.7. A brief description of the procedural parameters such as the composition (nominal), calcination temperature (A = Calcination temperature of 500 ºC; B = Calcination temperature of 275 ºC) and number of impregnation steps of the catalysts. The catalysts were synthesized to achieve a nominal metallic loading of wt%= [10%;14%;17.5%]. All catalysts described in Table S.7, were prepared by impregnating $Co(NO_3)_3 \cdot 6H_2O$ over γ-Al_2O_3.

Characterization

SEM:

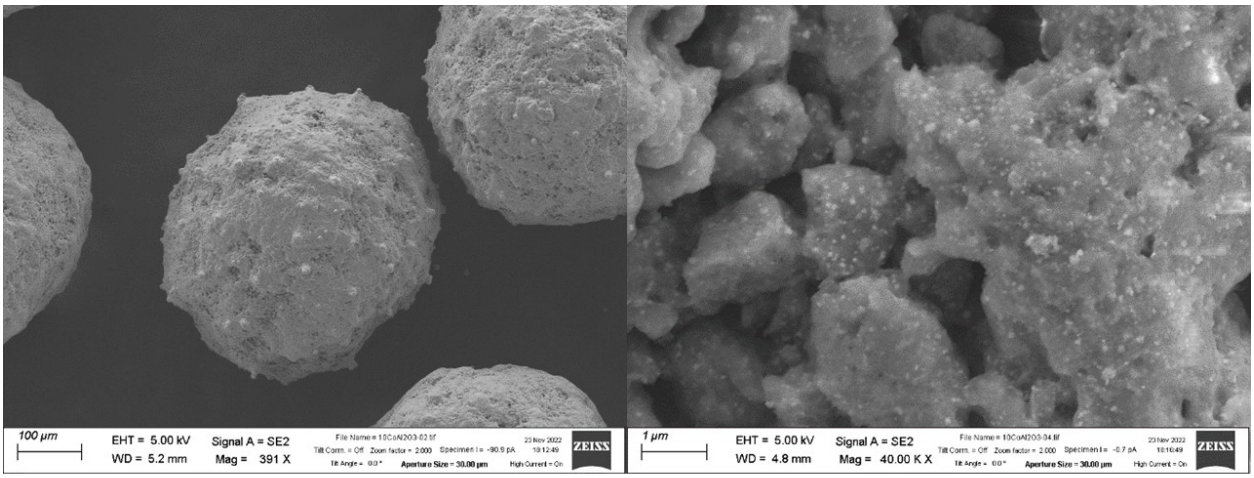

Figure S.17: SEM image of the 10A Catalyst pellet.

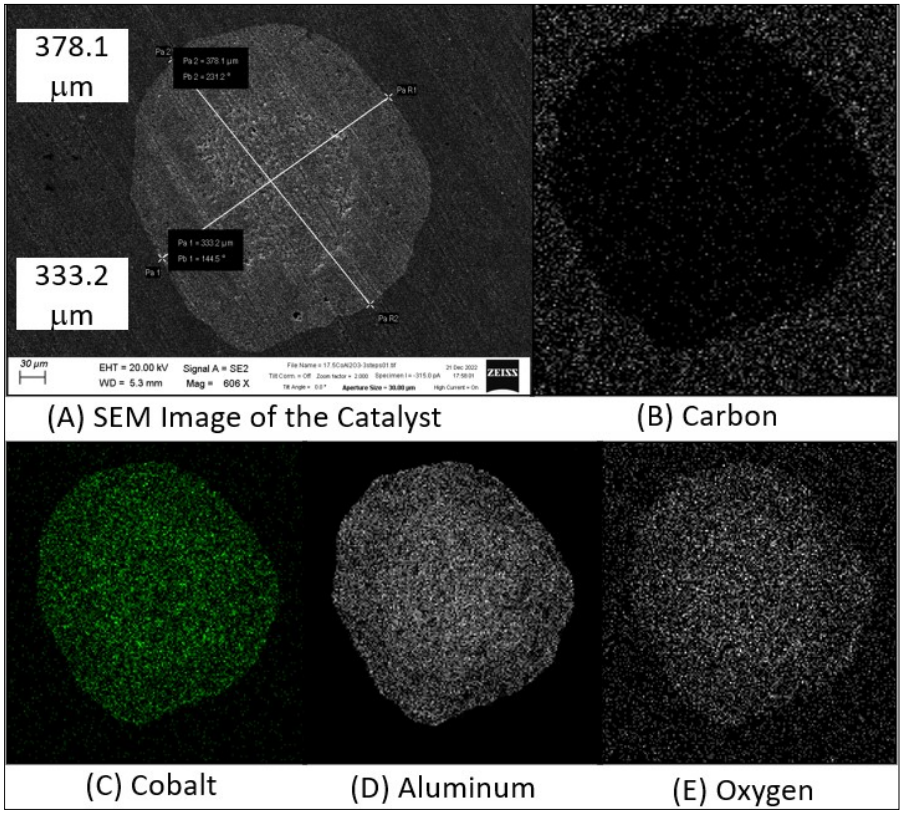

Figure S. 18: Cross-section of a catalyst particle (17.5A3)(A) SEM micrography of the particle; (B) EDX of Carbon atoms; (C) EDX of cobalt; (D) EDX of Aluminum atoms; (D) EDX of oxygen.

Density and ICP:

Table S.13: Skeletal density and chemical composition of synthesized catalysts.

Cat. ID	Wt.% ICP Cobalt	Real Density [kg/dm^3]
10A	9.20	3.28
10B	8.60	3.27
14B	10.80	3.33
14A	11.55	3.35
17.5A1	16.00	3.46
17.5A3	15.40	-
17.5Bi	14.65	3.39
17.5B1	15.20	3.43
□-Al_2O_3	0	3.27

N_2-physisorption:

Table S.14: Surface area and mesopore volume of catalysts

Cat. ID	S_{BET} (m^2/g)	V_{meso} (cm^3/g)
10A	152	0.48
10B	176	0.52
14B	161	0.50
14A	150	0.49
17.5A1	144	0.45
17.5A3	162	0.49
17.5Bi	168	0.49
17.5B1	151	0.44

XRD:

Table S.15: Particle size and FWMH of catalysts.

Cat. ID	FWMH (º)	D (nm)
10A	0.16	53
10B	0.315	27
14B	0.472	18
14A	0.276	30
17.5A1	0.354	24
17.5A3	0.315	27
17.5Bi	0.576	15
17.51	0.315	27

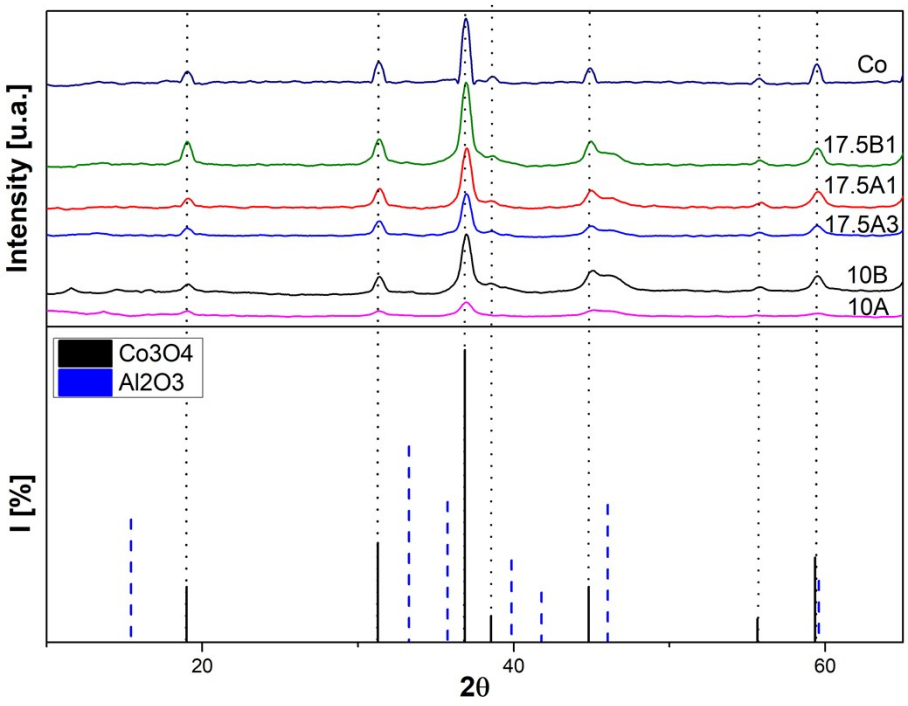

Figure S.19: XRD diffractograms of the non-promoted catalysts used in this work prior to reduction.

TPR:

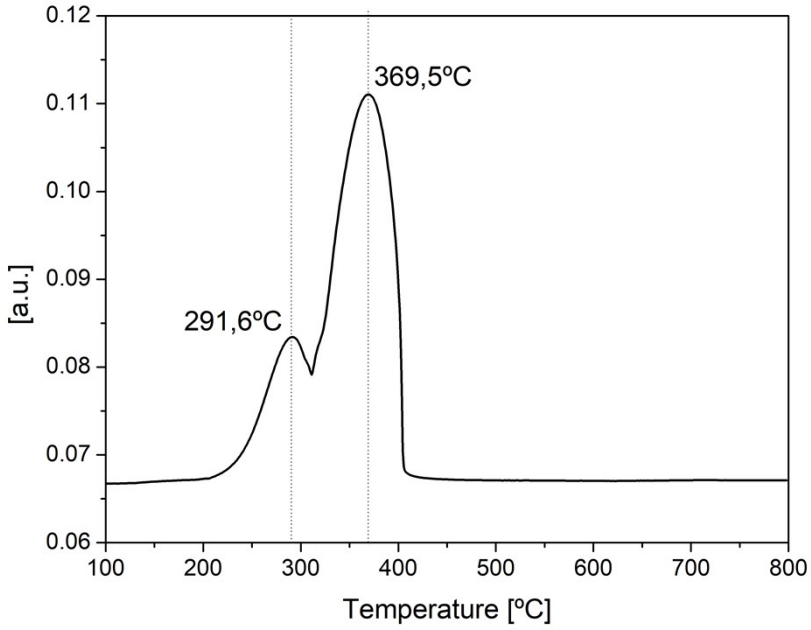

Figure S.20: TPR profile of the non-supported cobalt oxide calcined at 500ºC.

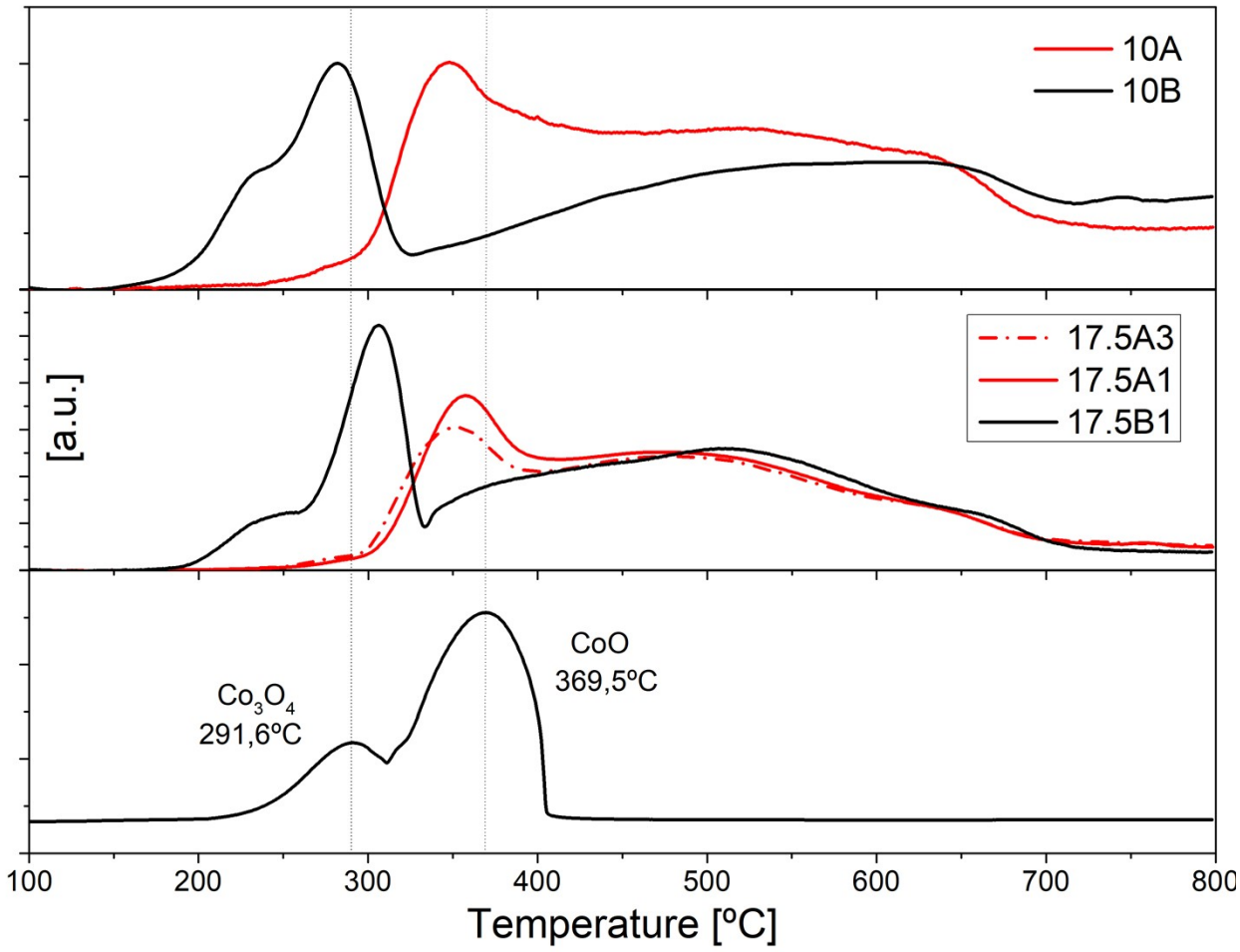

Figure S.21: Comparison of catalysts TPR.

CO Chemisorption:

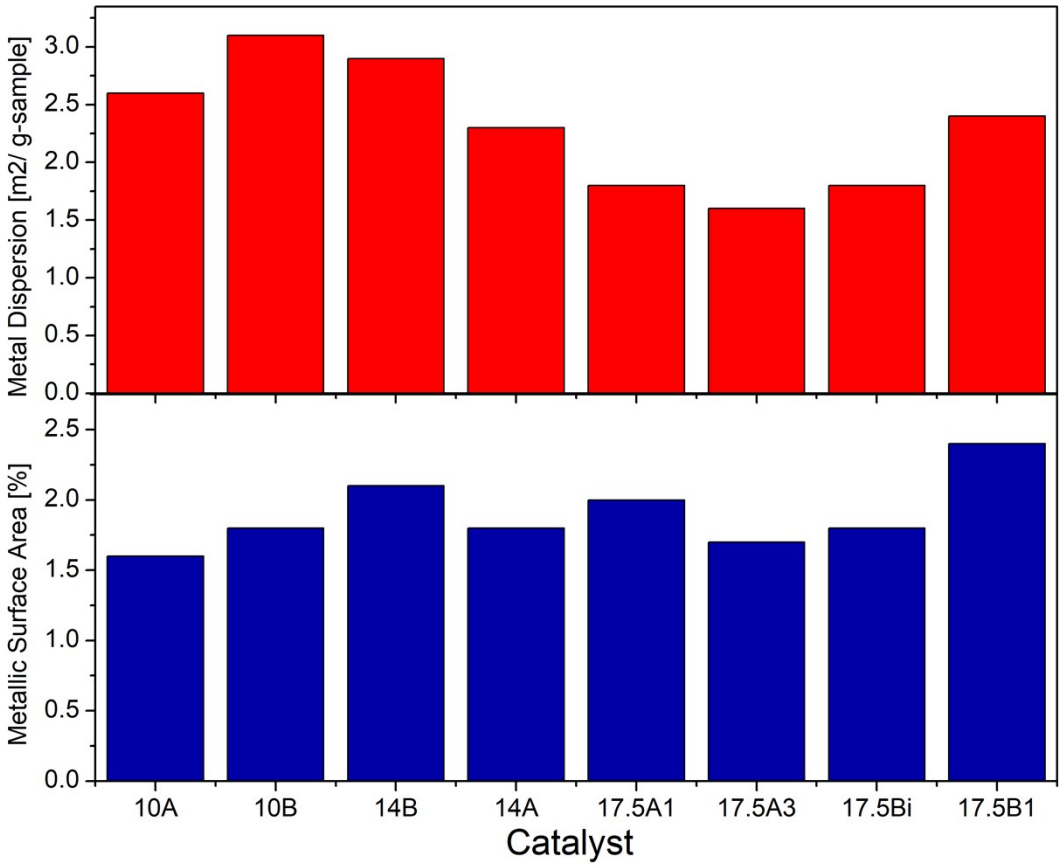

Figure S.22: Metallic Surface Area and Metallic Dispersion measured by CO Chemisorption.

Catalytic Results

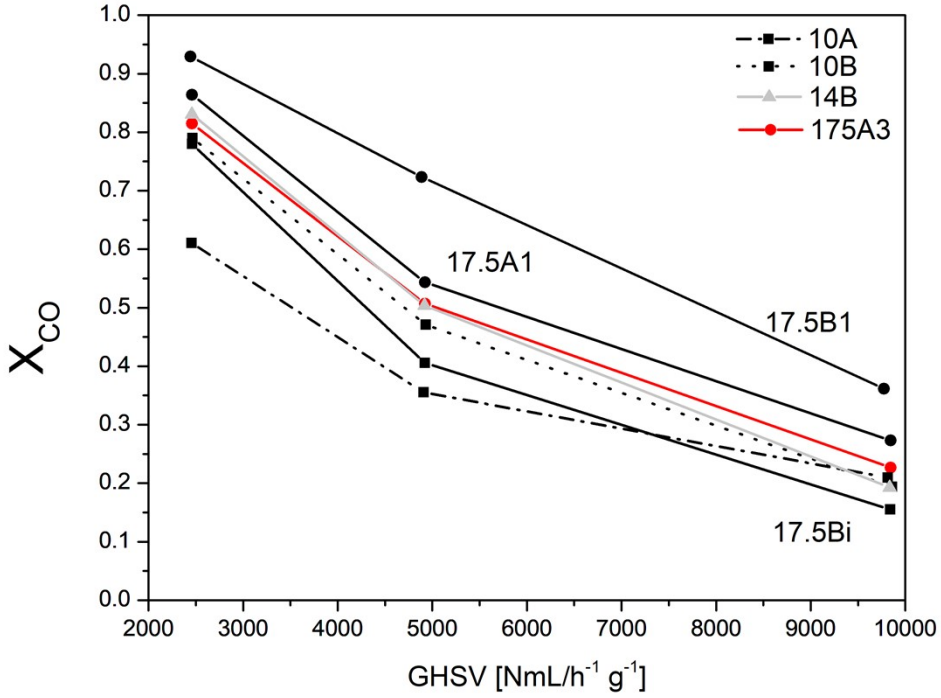

Figure S.23: : CO Conversion of the catalyst at different GHSVs.

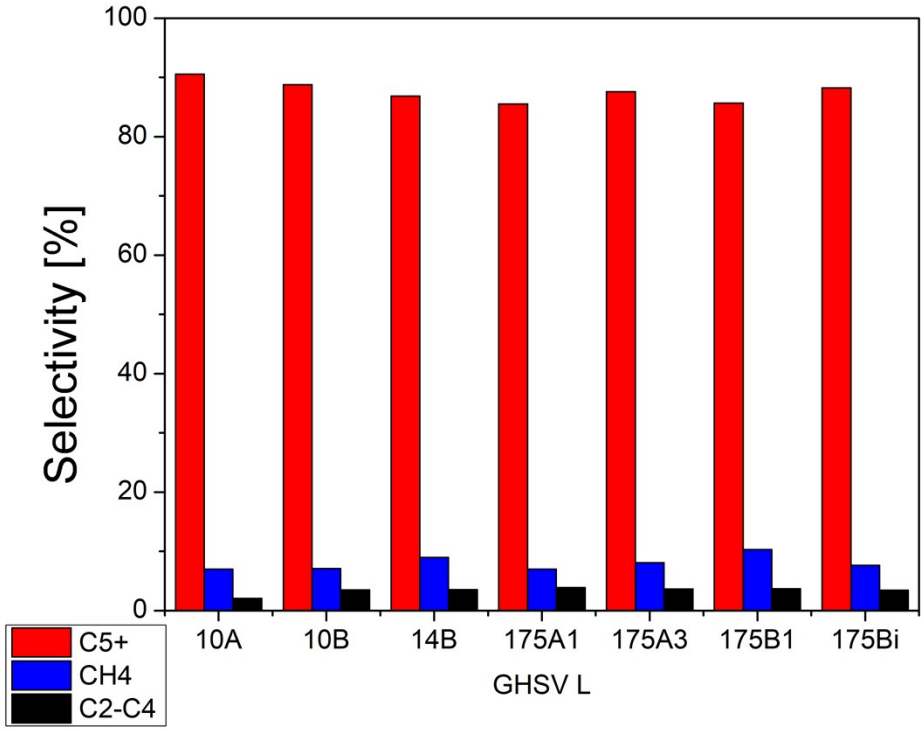

Figure S.24: Selectivity at low GHSV.

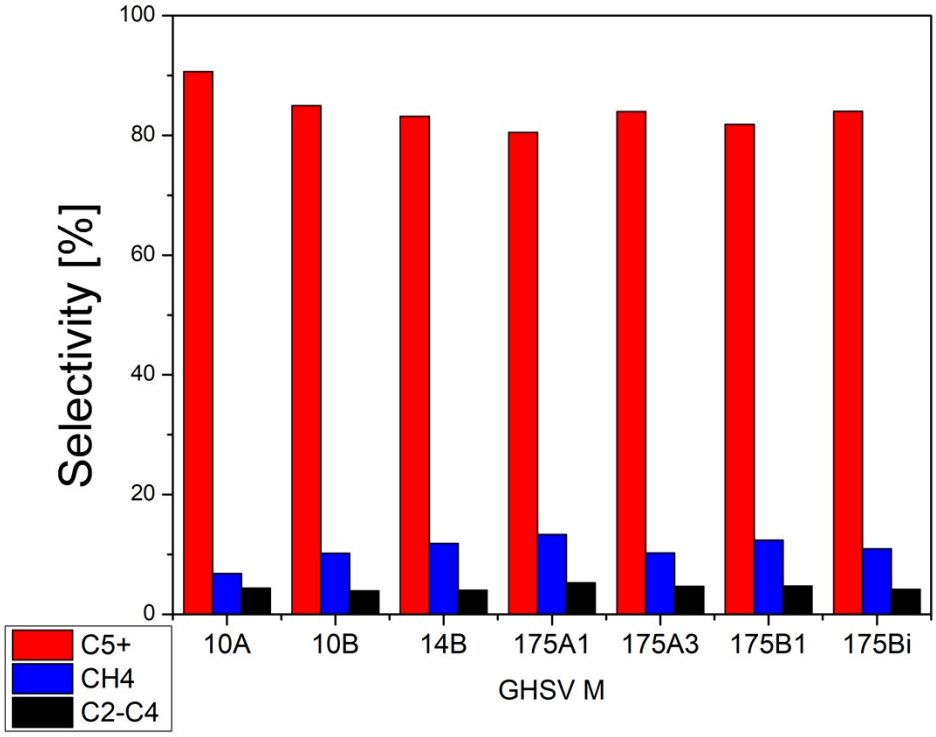

Figure S. 25: Selectivity at medium GHSV.

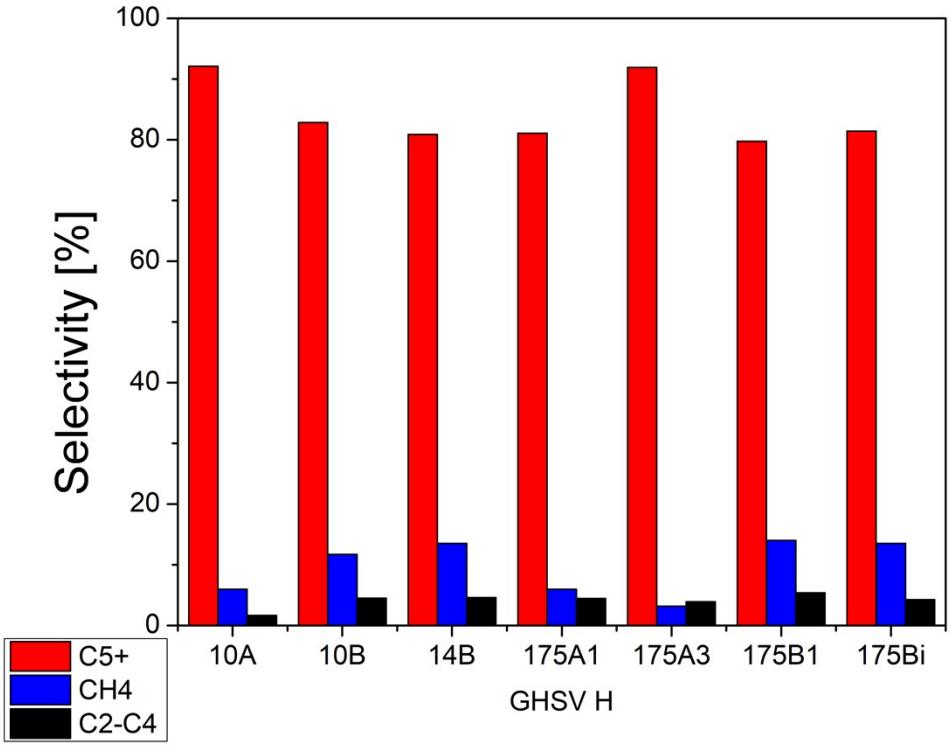

Figure S. 26: Selectivity at high GHSV.